

Metal and Slag Extraction from Different Zones of a Submerged Arc Furnace with Non-uniform Porous Bed Using CFD



Varun Loomba, Jan Erik Olsen, and Kristian Etienne Einarsrud

Abstract A submerged arc furnace (SAF) is generally used in the production of ferroalloys (referred to as metal in this study). Viable production of ferroalloys requires a consistent tapping process where metal and slag are extracted from the furnace. The tapping flow rates depend on various in-furnace conditions such as the height of the metal and slag column, presence of a porous coke bed (particle bed), crater pressure, and the physical properties of the fluids. In order to understand the difference in drainage of metals and slags produced in different zones of the furnace, a computational fluid dynamics (CFD) study is performed. Variations in the tapping of metal and slag from the different zones would lead to accumulation in the furnace, thus reducing its efficiency. A comparison between the tapping rates for the metal produced in the front or the back zone of the furnace is performed for a uniformly distributed coke bed and a coke-free bottom region. The tapping rates of slag produced in different zones of the furnace for a uniformly distributed particle bed are also compared. The results showed that the furnace reached a quasi-steady state quicker for the coke-free bottom region compared to the uniformly distributed particle bed, whereas the tapped metal comes equally from all zones of the furnace. It took longer for the simulation to reach a quasi-steady state for extraction of slag produced in different zones due to higher initial volume of slag. At the quasi-steady state, the slag was tapped equally from all zones of the furnace.

Keywords CFD · Porous media flow · Tapping · Furnace simulation

V. Loomba · K. E. Einarsrud (✉)
Department of Material Science and Engineering, NTNU, Trondheim, Norway
e-mail: kristian.e.einarsrud@ntnu.no

V. Loomba
e-mail: varun.loomba@ntnu.no

J. E. Olsen
Process Technology Group, SINTEF AS, Trondheim, Norway
e-mail: jan.e.olsen@sintef.no

Introduction

Efficient furnace operation depends on several factors where one of the crucial processes is tapping i.e., extraction of the molten metal and slag from the furnace. Poor tapping could lead to metal and slag accumulation in the SAF, reducing the efficiency of the entire process. The metal and the slag drain out of the furnace due to gravity, therefore their flow rates depend on the height of the liquid column accumulated in the furnace. In batch tapping, the tap-hole is opened when a significant amount of metal and slag have accumulated in order to facilitate their flow out of the furnace. The unreacted coke particles in the furnace hinder the flow of the metal and the slag by offering resistance to the flow, lowering their flow rates. It is not clarified whether the coke bed floats on top of the metal, the coke bed forms a bridge due to interlocking between the particles, or this observation is caused by a phenomenon occurring after the furnace shuts down. Regardless of the reason for the absence of a coke bed at the furnace bottom, it is worthwhile to verify if this affects the flow of metal and slag towards the tap-hole. Experimentation on the furnace tapping process is difficult due to the huge size and the extremely high temperatures at which the furnace operates. Computational fluid dynamics (CFD) is an excellent tool to study these kinds of processes without dealing with extreme industrial conditions.

CFD has previously been used intensively in the metallurgical industry to simulate the flow of metals and slags under various operational conditions, to understand various aspects of the tapping process [1–8]. In some studies, a uniform distribution of the particle bed has been considered [1–4], whereas others considered the presence of a coke-free region at the bottom of the furnace [5–8]. Further details of several studies implementing CFD for tapping process in SAF have been described by Bublik et al. [9].

The tap-hole is generally present on one side of the furnace, therefore the metal and the slag produced in the other side must travel through the entire furnace in order to be tapped. If remained untapped, the metal and the slag will consume some volume which will not be utilized for production, lowering the process efficiency. Therefore, in this study the extraction of the metal and the slag from different zones of the furnace is studied to better understand the accumulation of the fluids. Our previous study (Loomba et al. [10]) includes the effect of uniform and a non-uniform distribution of particle bed inside the furnace on the tapping flow rates of the metal produced in different zones of the furnace. A comparison of the metal tapping flow rate produced in the back of the furnace relative to the metal from the front of the furnace has been shown in detail. In this paper, we continue the research to include the coke-free bottom region to study the metal tapping rates produced in different zones of the furnace relative to the metal from the front. Further, the extraction of slag from different zones of the furnace is also considered.

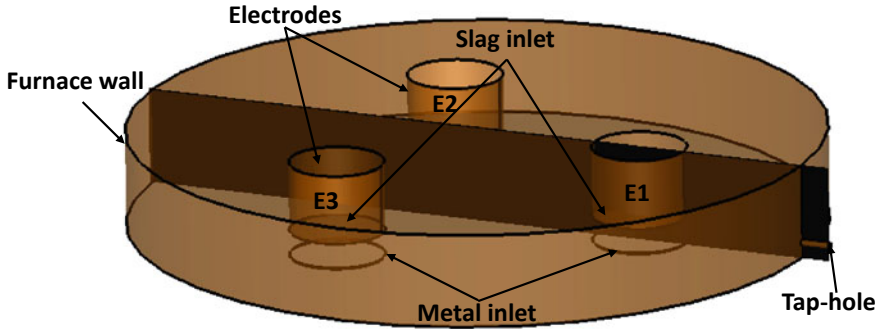


Fig. 1 Furnace design describing the different parts. The plane is used for analysis of metal and slag volume fractions in the results section

Materials and Methods

All flows can be mathematically represented by the Navier–Stokes equations [11], which are a set of partial differential equations describing the velocity of a fluid in all directions, including all the physical processes that facilitate the flow. These equations cannot be solved analytically for complex flow systems, which is the case in most flow systems. Computational Fluid Dynamics (CFD) is a technique to solve these equations numerically for all possible flow situations [12].

The simulated furnace in this study is an industrial-scale furnace, 10 m in diameter and 4 m high which represents a ferromanganese (FeMn) furnace. Since all the liquids are present in the bottom part of the furnace, only 1.5 m height is considered in the simulations. The furnace consists of three electrodes (E1, E2, and E3) that generate an electric arc to heat the materials, but from the fluid dynamic purpose, they act as solid walls present 0.5 m above the base of the furnace. The tap-hole is present on one side of the furnace near one of the electrodes with a diameter of 0.1 m. The tap-hole is located 0.1 m above the bottom surface of the furnace. A square cross-section tap-pipe is considered in these simulations to improve the mesh quality. Figure 1 shows the schematic diagram with the location of each of the components. The metal and the slag inflow are calculated based on the production rates of 300 and 200 tonnes/day.

Simulation Setup

Three fluid phases (the metal phase, the slag phase, and the gas) are defined in the simulations. The metal being the densest forms the bottom layer followed by the slag and the gas forming the top layer. The physical properties of the fluids are specified in Table 1 [8]. Since there are three immiscible fluids in the furnace, a multiphase volume of fluid (VOF) approach is used in the simulations [13]. In this approach, the

Table 1 Physical properties of the fluids

Material	Density (kg/m ³)	Viscosity (Pa s)
Metal	6,100	0.005
Slag	3,000	0.1
Gas	1	1×10^{-5}

interface between each phase is tracked along with the velocity profile calculation. The metal and the slag are produced in the entire bottom part of the furnace but for the simulation purposes, slag inlet is defined on the bottom surface of the electrodes whereas three discs are defined on the bottom surface of the furnace under each electrode which serve as metal inlets as shown in Fig. 1. The furnace is divided into three zones, one under each electrode (E1, E2, and E3), in order to realize whether the metal (or slag) being tapped comes from which region of the furnace. To determine in which zone of the furnace the fluids being tapped are produced, a separate fluid phase (metal or slag) is defined in each zone in order to identify the tapped fluid (but with the same physical properties as in other zones). This is explained in detail in the following sections.

The geometry of the furnace was designed using Gambit 2.4.3 software and the simulations were performed in OpenFOAM[®]. MultiphaseInterFoam module of OpenFOAM[®] was used for these simulations which implements the VOF multiphase approach. The Navier–Stokes equations are solved in this method for calculating the velocity profiles which are shared by all the phases. Additional equations (derived from continuity equations) are solved to track the interface between the phases. Therefore, adding more phases leads to additional equations being solved, slowing down the simulations. The dam break tutorial in OpenFOAM was used as the basis to build up the model. The geometry and mesh, the boundary and initial conditions, and the physical properties of the fluids were replaced in order to define our case. Finally, a topoSet file was added to define the porous region and a fvOptions file was added to include the resistance from the particle bed.

Several real-time tapping and production periods were simulated, where each tapping period is 20 min long and the production period is 2 h long. There is no outlet during the production period and the fluids are accumulated in the furnace during this time. The fluids are symmetrically distributed in the furnace at the beginning, which is not the usual case, i.e., after a certain operational time, the metal (or slag) produced at the back of the furnace will reach the other zones of the furnace. Therefore, several tapping and production cycles are required to reach the quasi-steady state, i.e., when the ratio of mass flow rates of each metal and the slag does not vary significantly in successive taps.

Porosity Distribution

The unreacted coke particles form a porous particle bed creating a resistance to the flow of the metal and the slag. This additional resistance is added to the Navier–Stokes equations using the Ergun equation, added as a sink term thereby reducing the velocity of the fluids through the fvOptions methodology in OpenFOAM. The Ergun equation describes the pressure drop across the bed as a function of the properties, the fluid physical properties, and the flow properties as shown in Eq. 1:

$$-\frac{\Delta P}{L} = \frac{150\mu_f(1 - \varepsilon)^2}{d_p^2\varepsilon^3}u + \frac{1.75\rho_f(1 - \varepsilon)}{d_p\varepsilon^3}u^2 \quad (1)$$

where ε is the particle bed porosity, d_p is the particle diameter, μ_f and ρ_f are the fluid viscosity and density, and u is the fluid velocity. The negative sign in Eq. 1 signifies the pressure loss created by the particle bed. The first term of the equation describes the viscous pressure loss, and the second term includes inertial effects. The Ergun equation is reduced to the Kozeny–Carman equation when the second term in Eq. 1 is excluded. Several researchers in the metallurgical field have used the Kozeny–Carman equation for the flow through the porous bed, arguing that the flow is laminar for highly viscous fluids such as the metal and the slag, but Olsen and Reynolds [14] showed that better results were obtained when the Ergun equation is used instead of Kozeny–Carman equation. For most of the particle bed, the flow is laminar. However, in front of the tap-hole where liquids accelerate into the tap-hole, the flow becomes turbulent. This is important for pressure loss.

Simulation Cases

Two separate cases are simulated, one to determine the extraction of metal from different zones of the furnace and the other to determine the extraction of slag phase.

Base case: Extraction of metal from different zones of the furnace for uniformly distributed particle bed.

Three metal phases are defined under each electrode (named metal1, metal2, and metal3 corresponding to the electrodes E1, E2, and E3 from Fig. 1) and only one slag phase as the focus is on metal tapping, in order to speed up the simulations. The metal enters the furnace constantly whereas there is no slag inlet. The velocity of metal is defined at the inlet based on the production rate of the metal, and the amount of slag produced during each tapping and production period is added on top to have the same hydrostatic head. The atmospheric pressure is defined on the top surface of the furnace, and wall boundary conditions (no slip for velocity and no flux for pressure) are defined at the furnace walls, tap-hole pipe walls, and the slag inlet. The outlet boundary conditions change from pressure outlet (atmospheric

pressure) during tapping to wall boundary during the production period. A uniformly distributed particle bed is defined with a porosity of 0.45 and a particle diameter of 0.03 m. This case has been explained in detail in our paper Loomba et al. [10]. All the boundary conditions used in this simulation are shown in Table 2. A static adaptive mesh was used for the simulation with more number of elements in the bottom region where most of the flow is happening and fewer elements in the top region as it is covered by the gas. This allows the use of coarser mesh without compromising the accuracy of the results, in order to save the simulation time. Since several tapping and production simulations are required, the mesh cannot be extremely fine in order to constrain the simulation time, therefore 286,000 mesh elements were used for these simulations with minimum cell volume $1.455 \times 10^{-6} \text{ m}^3$, maximum cell volume $3.7 \times 10^{-3} \text{ m}^3$, and average cell volume $3.9 \times 10^{-4} \text{ m}^3$.

Case 1: Extraction of metal from different zones of the furnace with non-porous bottom region.

The previous case is extended to add a non-uniformity by adding a coke-free bottom region to the furnace. The particle bed is removed from the bottom of the furnace till the bottom of the tap-hole. The particle bed properties in the rest of the furnace are the same as in the base case. The boundary conditions and the mesh properties used for this case are the same as used in the base case and specified in Table 2. The initial distribution of the metal and the slag phases is shown in Fig. 2.

Case 2: Extraction of slag from different zones of the furnace.

In this case, three slag phases (named slag1, slag2, and slag3 corresponding to the regions below the electrodes E1, E2, and E3 from Fig. 1) and one metal phase are considered as the focus is on tapping of slag rather than metal. Both metal and

Table 2 Boundary conditions used in the simulation for the base case

Boundary	Tapping	Production
Metal inlet	Velocity inlet (calculated from production rates)	Velocity inlet
Slag inlet	Wall	Wall
Furnace wall	Wall	Wall
Outlet	Pressure outlet	Wall
Surface	Atmospheric pressure	Atmospheric pressure

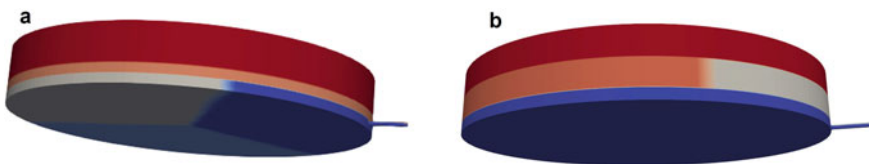


Fig. 2 **a** Case 1: 3 metal phases, 1 slag phase with non-porous bottom region and uniformly distributed porosity in the top region ($\epsilon = 0.45$ and $d_p = 0.03 \text{ m}$), **b** case 2: 1 metal phase, 3 slag phases with uniformly distributed porosity in the entire furnace ($\epsilon = 0.45$ and $d_p = 0.03 \text{ m}$)

Table 3 Boundary conditions used in the simulation of case 2

Boundary	Tapping	Production
Metal inlet	Velocity inlet (calculated from production rates)	Velocity inlet
Slag inlet	Velocity inlet (calculated from production rates)	Velocity inlet
Furnace wall	Wall	Wall
Outlet	Pressure outlet	Wall
Surface	Atmospheric pressure	Atmospheric pressure

slag inlets are defined in this case, metal from the disc at the bottom (as in previous cases) and the slag from the bottom surface of the electrode wall. The initial amount of slag in this case is double that of the previous cases such that the slag level in the furnace should always remain above the height of the slag inlet, in order to avoid any divergence in the solution. Particle bed is uniformly distributed, the same as the base case. Figure 2 shows the metal and the slag distribution in each case. The slag inlets are defined with a velocity calculated from the mass production rate of the slag (similar to metal inlet velocity). All other boundary conditions used are the same as in the base case. Table 3 shows the list of boundary conditions used for these simulations. The initial level of the slag in the furnace is higher in this case than in the previous case, therefore a coarse mesh cannot be used in the top region of the furnace, hence 722,000 mesh elements were used in this case: minimum cell volume $1.25 \times 10^{-6} \text{ m}^3$, maximum cell volume $7.3 \times 10^{-4} \text{ m}^3$, and average cell volume $1.56 \times 10^{-4} \text{ m}^3$.

Results and Discussion

Simulations were performed using an open-source CFD software called OpenFOAM® version 7 [15], whereas plotting was performed in Matlab [16].

Flow Profiles

The flow patterns of all cases are similar. Figure 3 shows the volume fractions of each phase for all cases at the beginning of the first tap and at the end of the fourth tap. The plane shown in Fig. 3 passes through the middle of the tap-hole and perpendicular to the base of the furnace (as shown in Fig. 1). On the backside of the furnace, this plane passes through the interface between metal2 and metal3 (or slag2 and slag3). On opening the tap-hole, the fluids start flowing out of the furnace due to the hydrostatic pressure of the accumulated liquid column in the furnace. The initial level of the metal is above the tap-hole, therefore only metal should flow out of the furnace in the beginning until the metal–slag interface reaches the tap-hole height,

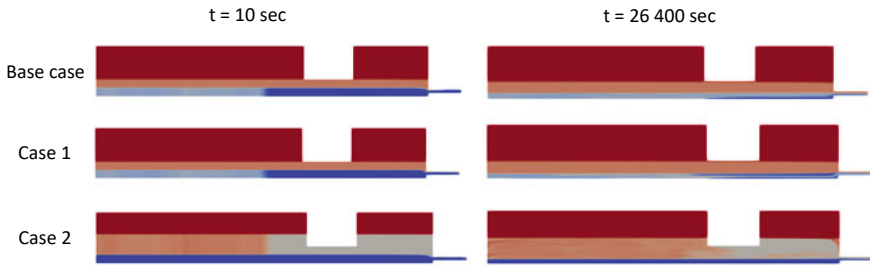


Fig. 3 Volume fraction along the plane perpendicular to the base of the furnace, passing through the center of the tap-hole (as shown in Fig. 1) for both cases at 10 s (tap 1) and 26,400 s (tap 4) from the beginning

but the metal–slag interface near the tap-hole bends due to the high viscosity of the slag and the slag also flows out from the beginning. This is evident from the first column in Fig. 3a where the bending of the metal–slag interface is visible even 10 s after opening the tap-hole. As metal1 covers the region near the tap-hole in the base case and case 1, only metal1 is tapped in the beginning whereas metal2 and metal3 come closer to the tap-hole. Since the bottom region (where metal1, metal2, and metal3 are produced) is free of particle bed in case 1, the metals flow faster than the base case with particle bed at the bottom of the furnace. Therefore, metal2 and metal3 also start flowing out towards the end of the first tap in case 1. It takes two taps for metal2 and metal3 to reach the tap-hole and be tapped for the base case due to the resistance by the particle bed. At the end of the fourth tap (second column in Fig. 3), it can be seen that metal2 and metal3 have been tapped for both cases. Similarly, slag1 covers the region near the tap-hole in case 2 and it starts flowing at the beginning of the first tap. The slag is always passing through the particle bed and due to the higher viscosity of the slag, the resistance offered to the slag is also higher compared to the metal. Since the slag has much higher volume in case 2 compared to the other cases, more number of taps are required for the slag at the back of the furnace to reach the tap-hole. Therefore, even at the end of the fourth tap (the second column in Fig. 3), most of the region near the tap-hole is still covered by slag1, and only small amounts of slag2 and slag3 are visible in the tap-hole pipe. This shows that more number of taps will be required for the furnace to reach the quasi-steady state for case 2 compared to the other cases.

Mass Extracted in Each Tap

Figure 4 shows the comparison of the tapped mass of each metal phase in each tap for the base case and case 1. Metal2 and metal3 are not tapped in the first tap for the base case as the region near the tap-hole is covered by metal1. In case 1, however, metal2 and metal3 are tapped even in the first tap because the metal phases

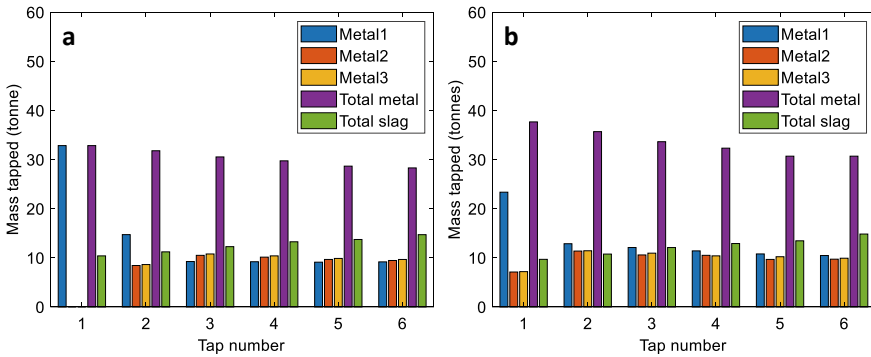


Fig. 4 The mass of metal1, metal2, metal3, and the slag phase in each tap for **a** the base case and **b** case 1

are moving faster in the absence of the resistance offered by the particle bed. The total amount of metal tapped in each tap is also larger for case 1 compared to the base case, due to fast-moving metal in the bottom region of the furnace, but it will become constant if the simulations run for longer times due to mass conservation. The total amount of slag tapped is similar for the base case and case 1 because the slag phase is always flowing through the particle bed in both cases. It is also evident that it takes at least three taps for the furnace to reach a quasi-steady state, after which the ratios of metal1, metal2, and metal3 remain constant for the subsequent taps, and only two taps are required for case 1. This again can be explained by the fast-moving metal at the bottom region of the furnace; the metal from the back can reach the tap-hole faster compared to the base case. At quasi-steady state, the amounts of metal1, metal2, and metal3 extracted are similar for case 1 signifying that once the furnace reaches its steady state, metal extracted in each tap comes equally from all zones of the furnace and not just the metal produced in the region near the tap-hole. Table 4 shows the amounts of each of the metal phases and the slag phase extracted in each tap for case 1. It can be confirmed from Table 4 that the amounts of metal1, metal2, and metal3 tapped become constant from the second tap onwards signifying that the furnace has reached the quasi-steady state. A significant amount of metal2 and metal3 are extracted in the first tap compared to only metal1 being extracted for the base case. The amounts of all three metal phases extracted become constant in the

Table 4 Mass of metal and slag extracted in each tap for case 1 in kg

Material	Tap 1	Tap 2	Tap 3	Tap 4	Tap 5	Tap 6
Metal1	23,370	12,875	12,104	11,417	10,797	10,474
Metal2	07,116	11,382	10,590	10,512	09,681	09,730
Metal3	07,194	11,442	10,955	10,405	10,227	09,924
Total metal	37,680	35,699	33,650	32,335	30,705	30,128
Slag	09,696	10,769	12,099	12,916	13,468	14,846

second tap for case 1 compared to the third tap in the base case. The fast movement of the metal in the porous free zone leads to the shorter time required for reaching the quasi-steady state.

As mentioned, earlier the initial amount of slag in case 2 is double that of the base case, therefore more taps are required for the furnace to reach the quasi-steady state. Figure 5 shows the comparison between the base case and case 2. In the first three taps, only slag1 is tapped because a larger volume of slag1 is covering the region near the tap-hole compared to the base case. Slag2 and slag3 start flowing out from the fourth tap, and it takes at least seven taps to reach the quasi-steady state compared to three taps in the base case. In the first three taps, the total slag tapped is equal to the amount of slag1 tapped. Once the furnace reaches the quasi-steady state, the amounts of slag1, slag2, and slag3 tapped are similar. The total amount of slag extracted in each tap is higher for case 2 compared to the base case and case 1 because of the higher hydrostatic head of the liquid column in case 2. A similar pattern occurs for the total metal extracted in each tap due to the same reason (Table 5).

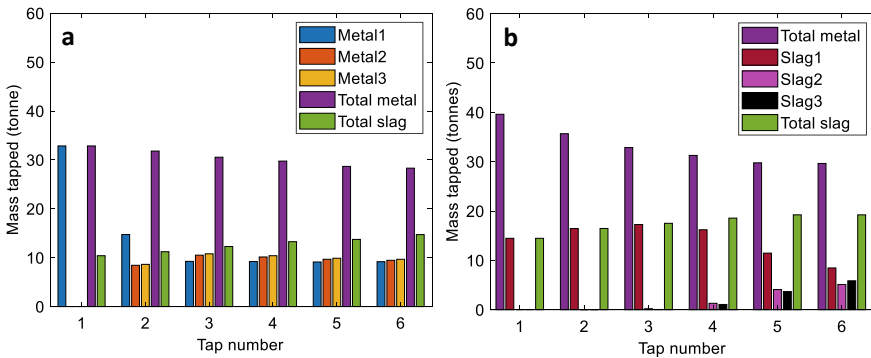


Fig. 5 The mass of different metal and slag phases in each tap for **a** the base case and **b** case 2

Table 5 Mass of metal and slag extracted in each tap for case 2 in kg

Material	Tap 1	Tap 2	Tap 3	Tap 4	Tap 5	Tap 6
Metal	39,606	35,669	32,862	31,266	29,766	29,641
Slag1	14,471	16,451	17,259	16,197	11,466	08,465
Slag2	0	6	112	01,298	04,083	05,118
Slag3	0	13	138	01,064	03,675	05,856
Total slag	14,471	16,469	17,509	18,560	19,225	19,441

Mass Flow Rate of Individual Metal and Slag Phases in a Single Tap

It can be inferred from the previous sections that the amount of each metal and slag phases extracted in each tap is constant once the furnace reaches a quasi-steady state. The mass flow rates of the metal and slag phases also become constant once the quasi-steady state is reached. Figure 6 shows the fifth tap for the three cases when the furnace has reached the quasi-steady state for the base case as well as case 1 and not yet for case 2. More taps are required for case 2 to reach the quasi-steady state. For the base case, metal1 (which is produced under the electrode E1) forces metal2 and metal3 from the previous tap present near the tap-hole to be tapped first, therefore peaks are seen in their mass flow rates at the beginning of the tap. The flow of metal1 is hindered by the particle bed leading to a time-lag in the extraction of metal1. The tapping flow rate increases for the metal1, once it reaches the tap-hole, whereas the tapping flow rate for the other two metal phases decreases. Towards the end of the tap when most of metal1 is tapped, its flow rate starts decreasing and allowing the other metal phases to be tapped. A similar flow profile to the base case is also observed in case 1 with a difference that the peaks for each of the metal phases appear sooner than the base case. The peaks have higher amplitude and lower standard deviation than the base case because of the resistance-free flow of the metal phases. The total amount of metal1 (calculated by integrating the curve in Fig. 6) extracted is slightly higher for case 1 compared to the base case, due to its fast movement, whereas the amounts of metal2 and metal3 are similar. When most of metal1 is tapped, its tapping flow rate starts decreasing and the tapping flow rates of metal2 and metal3 start increasing. The tapping rates of the slag are the same for both case 1 and the base case because the hydrostatic head is the same for both cases and the slag phase is always flowing through the particle bed, experiencing equal amount of resistance in both cases. The mass flow rates of metal1 dip down to a low value but not zero as some metal1 remains at the end of the tap. The mass flow rate profile of each of the slag phases in case 2 is similar to the total slag tapping flow rate in the base case and case 1 because a large amount of slag phases was assumed at the beginning of the first tap. The total slag tapped in case 2 is higher than the total slag phase in the

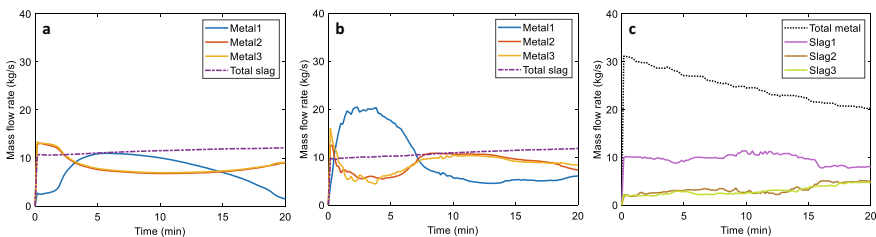


Fig. 6 The mass flow rates of the individual metal and slag phases for **a** the base case, **b** case 1, and **c** case 2 for the fifth tap

Table 6 Residence time (seconds) for individual metal and slag phases

Case	Metal1	Metal2	Metal3	Slag1	Slag2	Slag3
Base case	1,180	5,661	5,570	–	–	–
Case 1	1,643	4,284	4,139	–	–	–
Case 2	–	–	–	1,955	15,904	15,271

base case and case 1 because of the higher hydrostatic head. The total metal phase flow rate for case 2 is also higher than the base case (both have the same porosity distribution) due to the higher liquid column in case 2 leading to a higher hydrostatic pressure head.

Residence Time of Individual Metal and Slag Phases

The residence time of individual phases in the furnace is the average time spent by each phase inside the furnace. It can be quantified by considering the initial mass of each phase at the beginning of the tap, dividing it by the average mass flow rate of the respective phase. The residence time for each of the phases is shown in Table 6. The residence time for metal1 is less than metal2 and metal3 as the latter need more time to reach the tap-hole compared to metal1 which is formed closer to the tap-hole. The same pattern is seen for all three cases. The reason for higher residence time for metal1 and lower residence time for metal2 and metal3 for case 1 (porous free bottom region), compared to the base case, is the fast movement of the metal in the bottom region of the furnace. Metal2 and metal3 reach the tap-hole sooner, thereby substituting metal1 while tapping, compared to the base case. A similar trend is observed in the residence times for different slag phases in case 2; the residence time for slag1, slag2, and slag3 are 1,955, 15,904, and 15,271 s, respectively. These values are specified for the sixth tap, although the furnace has not reached the quasi-steady state yet. High values for slag2 and slag3 are observed because the initial volume of the slag is higher in case 2 compared to the other two cases and the furnace has not reached a quasi-steady state by the sixth tap. These values are shown in Table 6.

Conclusions and Outlook

A systematic numerical study of tapping of metal and slag from a SAF has been presented. The flow rate of the metal and the slag depends on the height of the liquid column accumulated in the furnace and the resistance offered by the particle bed to the flowing fluids. Three different cases have been discussed: the first is the base case with uniform porosity distribution in the furnace where metal extraction from different zones has been studied, in the second case the bottom region is a coke-free

region and the particle bed is uniformly distributed in the top part of the furnace, and the third case with similar porosity configuration as the base case but extraction of slag from different zones of the furnace is discussed. The main conclusion from this study is that the metal and slag produced in the back part of the furnace is extracted equally relative to the metal and the slag produced in the front side once the quasi-steady state is reached. The other following conclusions that can be drawn from this study are as follows:

- (1) The furnace reaches the quasi-steady state faster for case 1 (coke-free bottom region) compared to the base case (uniformly distributed porosity) in the furnace as the metal moves faster in the bottom region where there is no particle bed.
- (2) At steady state, the metal flows on average equally from all zones of the furnace, therefore there is no apparent accumulation of metal with the chosen porosity distribution for the furnace.
- (3) Similarly, the slag extracted at a quasi-steady state in case 2 (uniform porosity distribution) is also on average tapped in equal amounts from all zones of the furnace. It takes longer for the furnace to reach a quasi-steady state with respect to tapping of slag due to the higher initial amount of slag and the higher viscosity of slag as compared to metal.
- (4) When studying a single tap at a quasi-steady state, we see that the metal and slag produced at the electrode close to the tap-hole is drained first and then the products from the far electrodes towards the end. If the tap-hole is open sufficiently long, there will be an overall equal amount of tapping from each zone of the furnace.

In reality, there will be temperature gradients and cold spots where metal and in particular slag can solidify and accumulate. There is a higher likelihood for that to happen with metal and slag produced at the electrodes away from the tap-hole since these have longer residence times in the furnace than the metal and slag produced close to the tap-hole.

The methodology for predicting the tapping flow rates of metals and slags produced in different zones of the furnace has been presented. This can further be extended to include other non-uniformities that might be detected in the industrial furnaces. Further, it can be extended to calculate the shear stress on the furnace walls and thus the erosion of the furnace walls can be calculated. Once the flow profiles are calculated, the temperature profiles inside the furnace can be estimated by including the energy equation along with the flow equations.

References

1. Dash SK et al (2001) Optimum taphole length and flow induced stresses. *Ironmak Steelmak* 28(2):110–116
2. Dash SK et al (2004) Optimisation of taphole angle to minimise flow induced wall shear stress on the hearth. *Ironmak Steelmak* 31(3):207–215

3. Nishioka K, Maeda T, Shimizu M (2005) A three-dimensional mathematical modelling of drainage behavior in blast furnace hearth. *ISIJ Int* 45(5):669–676
4. Kadkhodabeigi M, Tveit H, Johansen ST (2011) Modelling the tapping process in submerged arc furnaces used in high silicon alloys production. *ISIJ Int* 51:193–202
5. Nishioka K, Maeda T, Shimizu M (2005) Effect of various in-furnace conditions on blast furnace hearth drainage. *ISIJ Int* 45(10):1496–1505
6. Guo BY et al (2008) CFD modelling of liquid metal flow and heat transfer in blast furnace hearth. *ISIJ Int* 48:1676–1685
7. Shao L, Saxén H (2012) Numerical prediction of iron flow and bottom erosion in the blast furnace hearth. *Steel Res Int* 83(9):878–885
8. Reynolds QG et al (2019) Phase effects in tap-hole flow—a computational modelling study. *J South Afr Inst Min Metall* 119(6):527–536
9. Bublik S et al (2021) A review of ferroalloy tapping models. *Metall Mater Trans B* 52(4):2038–2047
10. Loomba V, Olsen JE, Einarsrud KE (2021) Simulation of metal and slag in a Si-Mn furnace during production and tapping. In: *Infacon XVI*. Trondheim
11. Drazin PG, Riley N (2006) *The Navier-Stokes equations: a classification of flows and exact solutions*. London mathematical society lecture notes series. Cambridge University Press
12. Versteeg HK, Malalasekera M (2007) *An introduction to computational fluid dynamics: the finite method*, 2nd edn. Pearson Education Limited, Essex, England
13. Hirt CW, Nichols BD (1981) Volume of fluid (VOF) method for the dynamics of free boundaries. *J Comput Phys* 39:201–225
14. Olsen JE, Reynolds QG (2020) Mathematical modeling of furnace drainage while tapping slag and metal through a single tap-hole. *Metall Mater Trans B* 51(4):1750–1759
15. Foundation O (2020) OpenFOAM v7 user guide. <https://cfd.direct/openfoam/user-guide>
16. MATLAB, 9.7.0.1190202 (R2019b) (2019) Natick, Massachusetts